Electronic supplementary information (ESI)

# High-density monolithic pellets of double-sided graphene fragments based on zeolite-templated carbon

Atsushi Gabe[a], Mohammed Ouzzine[a,b], Erin E. Taylor[c], Nicholas P. Stadie[c], Naoki Uchiyama[d], Tomomi Kanai[d], Yuta Nishina[e], Hideki Tanaka[f], Zheng-Ze Pan[g], Takashi Kyotani[a], Hirotomo Nishihara[a,g]*

[a] *Institute of Multidisciplinary Research for Advanced Materials, Tohoku University, 2-1-1, Katahira, Aoba-ku, Sendai, 980-8577, Japan*

[b] *Department of Chemistry, Multidisciplinary Faculty of Beni-Mellal, University of Sultan Moulay Slimane, Av.Mghila, BP 592, 23000, Beni-Mellal, Morocco*

[c] *Department of Chemistry & Biochemistry, Montana State University, Bozeman, Montana, 59717, United States*

[d] *Atsumitec CO., Ltd. 7111, Yuto-cho, Nishi-ku, Hamamatsu-shi, Shizuoka 431-0192, Japan*

[e] *Research Core for Interdisciplinary Sciences, Okayama University, Tsushimanaka, Kita-ku, Okayama 700-8530, Japan*

[f] *Research Initiative for Supra-Materials (RISM), Shinshu University, 4-17-1 Wakasato, Nagano 380-8553, Japan.*

[g] *Advanced Institute for Materials Research, Tohoku University, 2-1-1, Katahira, Aoba-ku, Sendai, 980-8577, Japan.*

*Corresponding author. Tel: (+81) 22 217 5627,

E-mail: hirotomo.nishihara.b1@tohoku.ac.jp

## Preparation of ZTC

ZTC was prepared through the two-step process using zeolite Y (Na-form, $SiO_2/Al_2O_3 = 5.5$, obtained from Tosoh Co. Ltd.) as a template. Briefly, powdery zeolite Y was first dried at 200 °C under vacuum then impregnated with furfuryl alcohol at 0 °C in an ice bath under reduced pressure. After washing with mesitylene to remove furfuryl alcohol from the external surface of the zeolite powder, the furfuryl alcohol inside the zeolite channels was polymerized by heating the powder at 150 °C for 24 h. The resulting composite was then heated at 10 °C $min^{-1}$ under a flow of $N_2$ up to a temperature of 700 °C. When the temperature reached 700 °C, chemical vapour deposition (CVD) of propylene (4 vol.% in $N_2$) was accomplished for 2 h. After the CVD treatment, the zeolite/carbon composite was heat-treated at 900 °C for 3 h under a $N_2$ flow. Finally, the zeolite Y template was dissolved by HF treatment (47% aqueous solution), and the resulting liberated carbon was washed with copious amounts of water and air-dried at 120 °C overnight. The final carbon material, referred to as ZTC, is a powder made up of particles with submicrometer diameter.[1]

## Pelletization method

ZTC and GO in aqueous solution (10 mg $mL^{-1}$, NiSiNa materials Co. Ltd.) were mixed thoroughly to obtain a nominal GO/ZTC loading of 5 wt%. Distilled water was then added to the mixture followed by mixing again. After vigorous stirring, the so-obtained mixture was further mixed with a planetary mixing system at 2000 rpm for 10 min. Finally, this mixture was heated up to 60 °C to evaporate the water and hand ground into a homogeneous powder; this pre-pelletization dry mixture of ZTC and GO is referred to as ZTC_GO. Approximately 0.1 g of ZTC_GO was placed in a custom metal mold and hot-pressed under vacuum to a desired pressure and temperature, and held at the setpoint for 1 h. The resulting monolithic simples are referred to as ZTC_GO_TX_PY where X refers to the temperature setpoint and Y refers to the pressure setpoint during hot-pressing.

## Materials characterization

Electron spin resonance (ESR) analysis was performed using an electron spin resonance spectrometer (JES-X310) with a 9.542 GHz microwave frequency, 100 kHz modulation frequency, 1 mW power, and 2 min of sweep time. The samples (1 mg each) were sealed in 1-mm-internal-diameter, 50-mm-long quartz capillary tubes. Quantification of the number of unpaired spins was performed by comparison of the the ESR signal corresponding to 4-hydroxy-2,2,6,6-tetramethylpiperidine-1-oxyl (TEMPOL) and that of the sample, both in the presence of the same amount of Mn standard. Typically, $10^{-6}$ - $10^{-5}$ mol of TEMPOL or 1 mg of carbon was measured. The ESR peak area corresponds to the quantity of radicals, and of the signals measured for TEMPOL and the carbon samples were standardized based on the Mn standard.

The outer surface and cross-sectional morphologies of the pellets were investigated by scanning electron microscopy (Hitachi, S-4800) operating at 3.0 kV. The ordered structure of all samples was characterized by X-ray diffraction (XRD) with a powder X-ray diffractometer (Rigaku, MiniFlex600) using Cu Kα radiation. The ZTC/rGO pellets were cut using a spatula for diffraction experiments incident to the cross-section of the pellets.

The porous structure of all samples was characterized by $N_2$ physisorption at -196 °C using an automated adsorption system (BELMAX, BEL Japan) after degassing the samples at 150 °C under vacuum for 6 h. The adsorption kinetics were estimated by a manual approach with the same adsorption system (BELMAX, BEL Japan). Specifically, the sample tube containing a sample (sample weight was ca. 20 mg) was first evacuated until the pressure was less than 1 Pa. Then, ca. 300 Pa of $CO_2$ was introduced into the sample tube. After appropriate stabilization time (determined by a blank test, 20 s), the sample tube was isolated and the pressure within the sample tube was continuously monitored. High-pressure hydrogen adsorption measurements were performed with a volumetric Quantachrome device (iSorbHP) up to 100 bar at 25 °C. The density of compressed hydrogen gas ($d_{H2}$ [g cm$^{-3}$]) at the relevant temperature and pressure was obtained from the National Institute of Standards and Technology (NIST) website (http://www.nist.gov/): "Thermophysical Properties of Hydrogen" (https://webbook.nist.gov/cgi/fluid.cgi?Action=Page&ID=C1333740). Hence, the value of $M_{gas}$ [g g$^{-1}$] can be described as $d_{H2} \times V_{total}$. Lastly, stress-strain curves were measured with a Shimazu AUTOGRAPH AG-X plus apparatus.

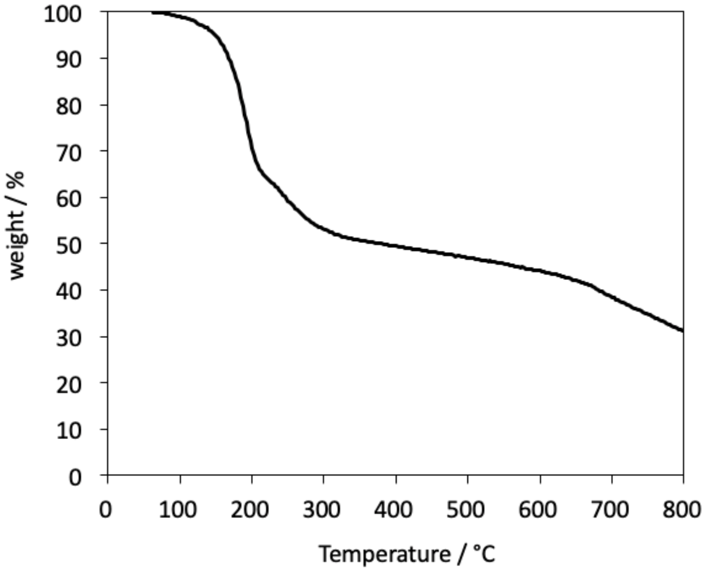

**Fig. S1** Thermal gravimetry (TG) of pristine GO under helium.

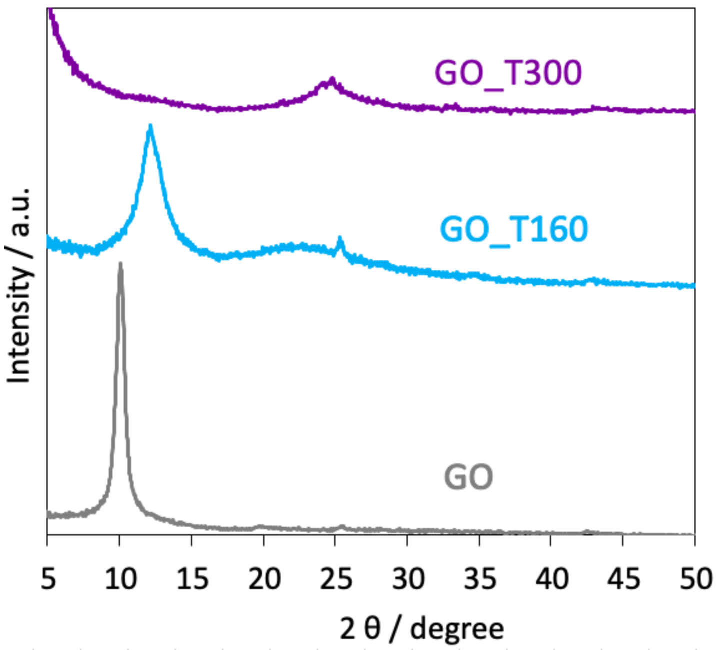

**Fig. S2** XRD patterns of GO before and after heat treatment at 160 °C and 300 °C without mechanical pressing for 1 h under vacuum.

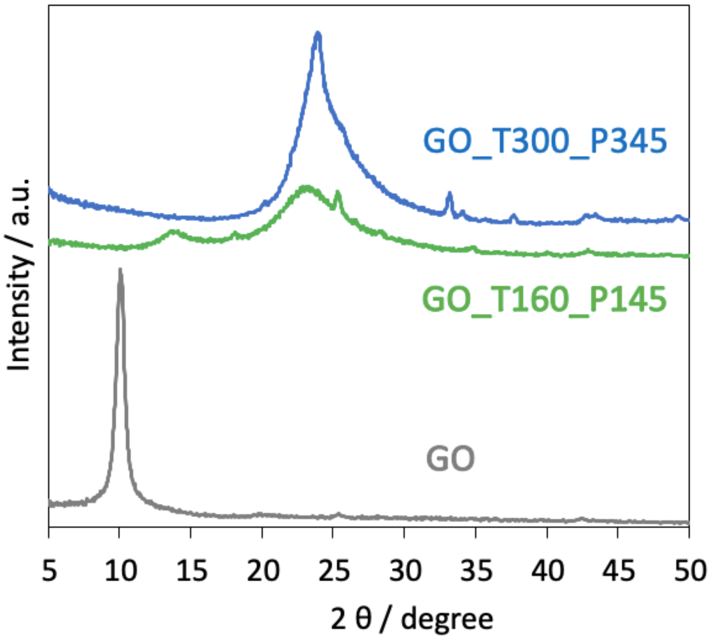

**Fig. S3** XRD patterns of GO before and after hot-pressing at 160 °C at 145 MPa and 300 °C at 345 MPa for 1 h under vacuum.

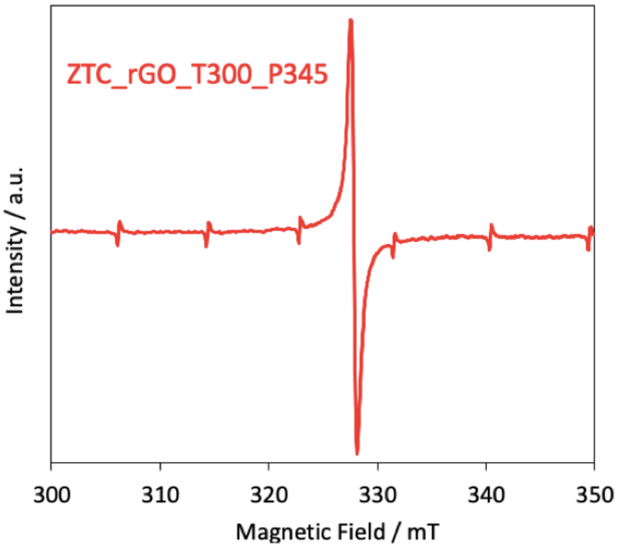

**Fig. S4** ESR spectrum of ZTC_rGO_T300_P345. The amount of unpaired spins is 1.5×$10^{16}$ $g^{-1}$.

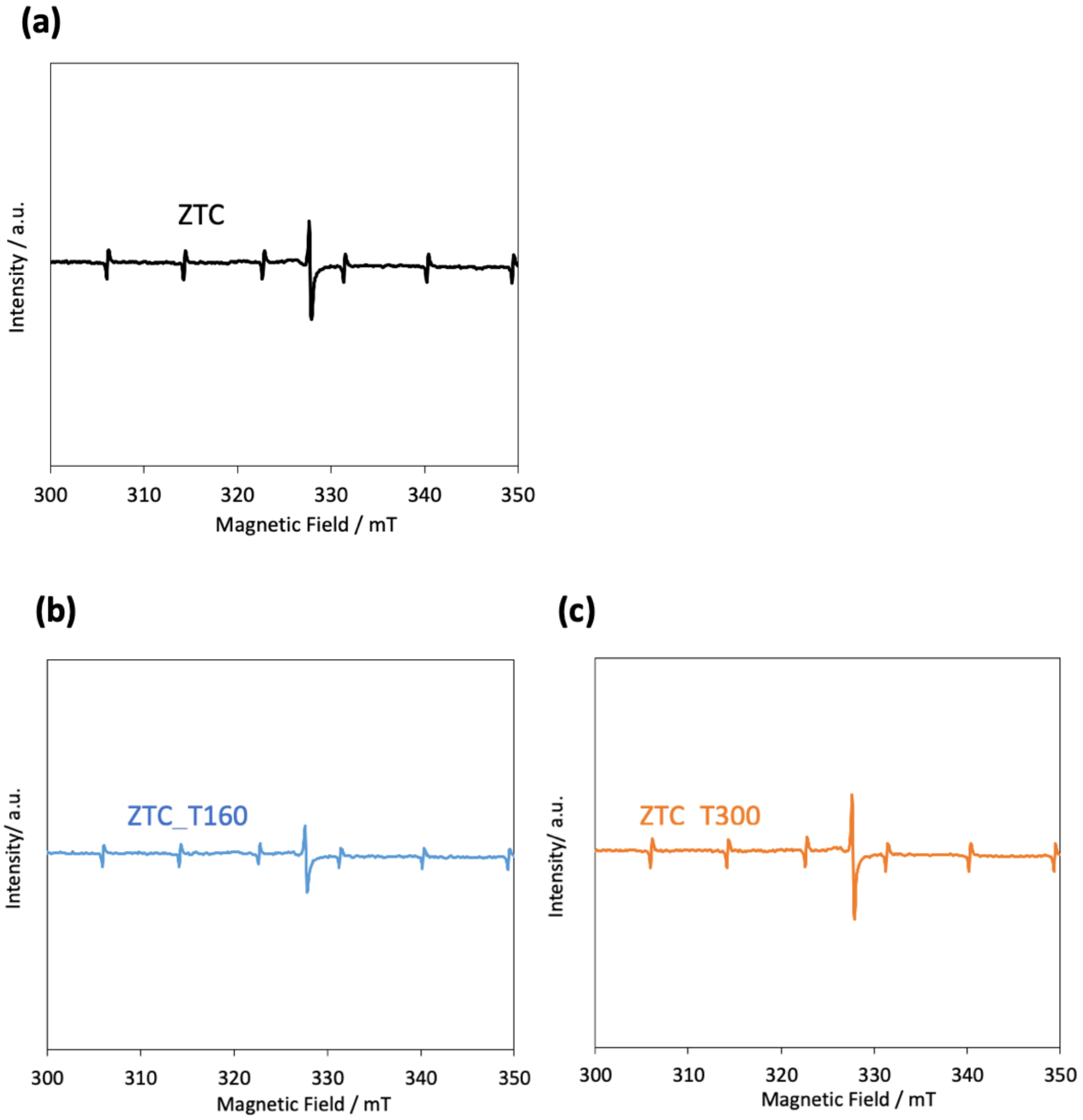

**Fig. S5** ESR spectra of ZTC powder before and after heat-treatment. (a) Pristine ZTC, (b) ZTC treated at 160 °C for 5 min, and (c) ZTC treated at 300 °C for 5 min. The amount of unpaired spins are (a) $3.3\times10^{15}$ $g^{-1}$, (b) $3.0\times10^{15}$ $g^{-1}$, and (c) $3.5\times10^{15}$ $g^{-1}$.

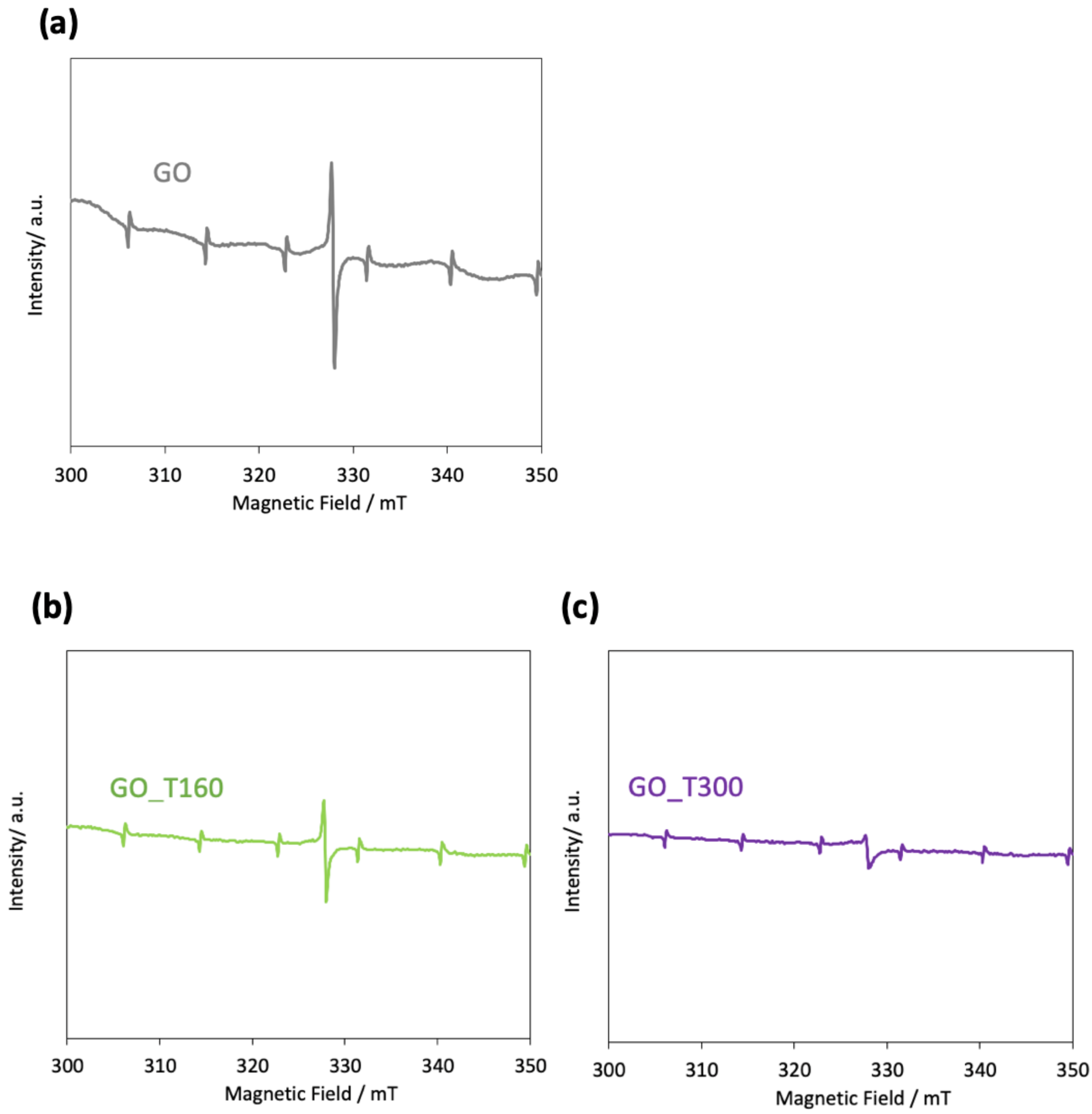

**Fig. S6** ESR spectra of GO before and after heat-treatment. (a) Pristine GO, (b) GO treated at 160 °C for 5 min, and (c) GO treated at 300 °C for 5 min. The amount of unpaired spins are (a) $1.7\times10^{15}$ $g^{-1}$, (b) $4.0\times10^{15}$ $g^{-1}$, and (c) $1.3\times10^{15}$ $g^{-1}$.

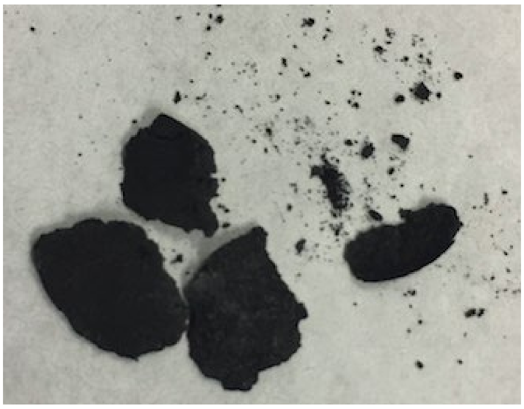

**Fig. S7** Photograph of the attempted densification of activated carbon (MSC-30) and GO for 160 °C at 345 MPa.

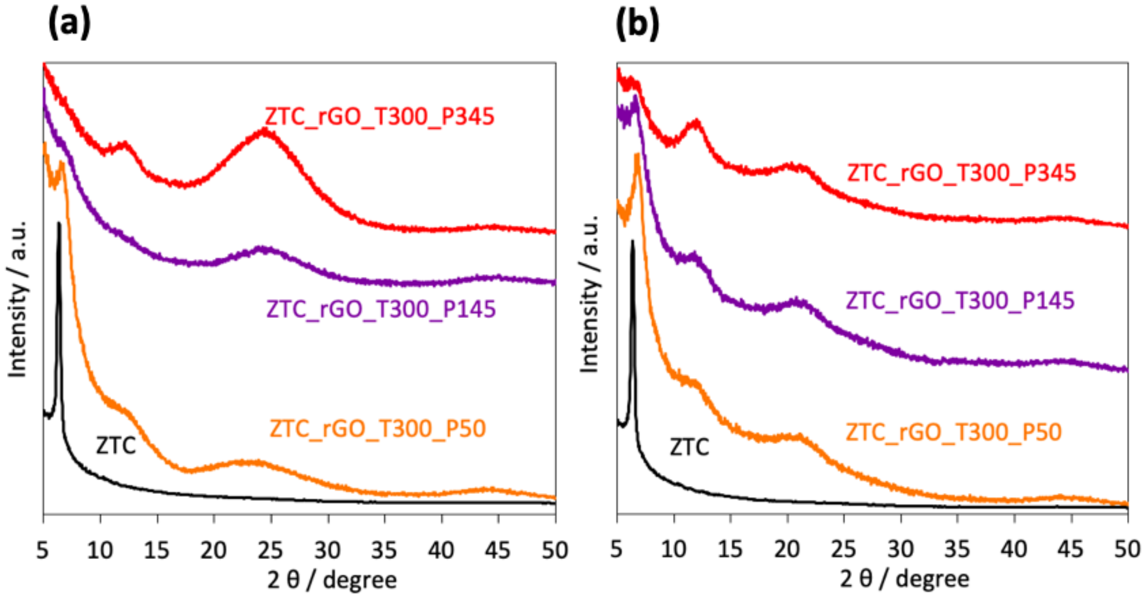

**Fig. S8** XRD patterns for (a) the pressed surface and (b) the cross-section of ZTC/rGO pellets prepared at 300 °C at several different pressures. The XRD pattern of the pristine ZTC powder is also shown for reference.

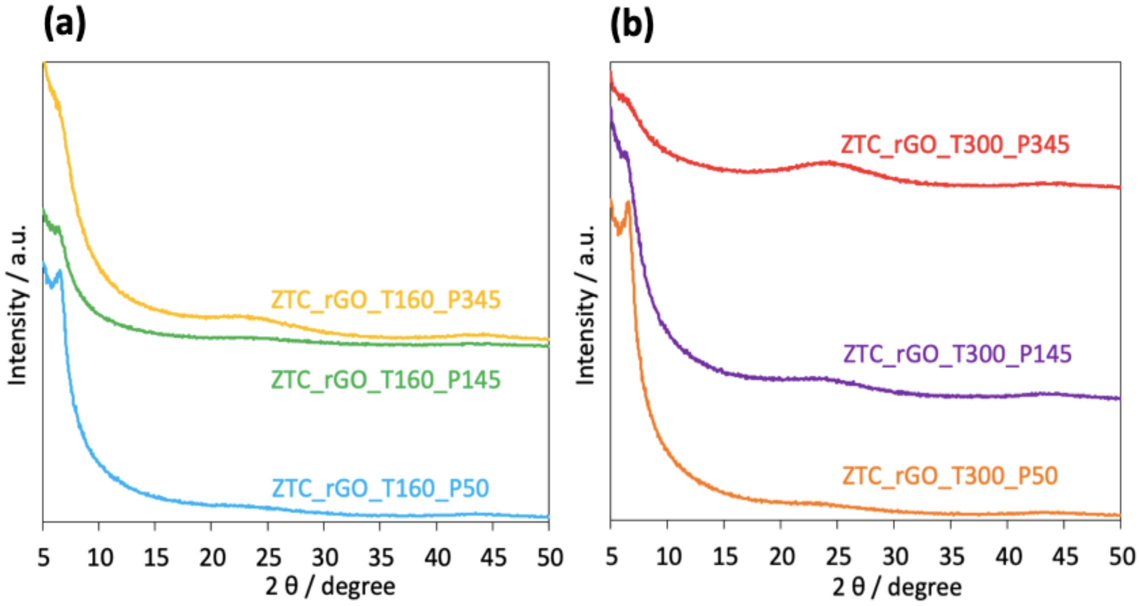

**Fig. S9** XRD patterns for pellets prepared at (a) 160 °C and (b) 300 °C, after grinding back into a powder.

**Table S1** Pore structure and density of carbon-based monolithic pellets reported elsewhere.

| $S_g$[a] /$m^2$ $g^{-1}$ | $\rho_{bulk}$[b] /g $cm^{-3}$ | $S_v$[c] /$m^2$ $cm^{-3}$ | Reference |
|---|---|---|---|
| 1586 | 0.80 | 1268 | [2] |
| 2147 | 0.42 | 902 | [3] |
| 2038 | 0.82 | 1671 | [4] |
| 1450 | 0.46 | 667 | [5] |
| 3183 | 0.50 | 1592 | [6] |
| 1975 | 0.44 | 869 | [7] |
| 2561 | 0.408 | 1044 | [8] |

[a] Surface area as determined by the BET method.

[b] Bulk density as determined from the pellet weight and hand-measured pellet volume.

[c] Volumetric surface area as determined from $S_g$ and $\rho_{bulk}$.

**Table S2** Physisorption-based hydrogen storage capacities in monolithic materials around room temperature.

| Material | Sample name | $W_{total}$ /g L$^{-1}$ | Conditions | Ref. |
|---|---|---|---|---|
| ZTC pellet | ZTC_rGO_T160_P145 | 10.5 | 25 °C, 100 bar | This work |
| Carbon pellet | M3M | 6.4 | 25 °C, 100 bar | [2] |
| Carbon pellet | A3-12 | 11.2 | 25 °C, 100 bar | [2] |
| Carbon pellet | ACNF-CD24 | 3.2 [a)] | 25 °C, 100 bar | [5] |
| Carbon pellet | ACNF-CD24M | 5.5 [b)] | 25 °C, 100 bar | [5] |
| Activated carbon fiber pellet | AXCF | 9.8 | 25 °C, 100 bar | [9] |
| Carbon pellet | AC | 8.9 | 25 °C, 100 bar | [10] |
| Carbon pellet | CM | 11 | 25 °C, 100 bar | [10] |
| MOF pellet | MOF-177<br>(>0.54 g cm$^{-3}$) | 3.2 ± 0.1 | r.t.[b)], 120 bar | [11] |
| MOF pellet | MOF-5+0% ENG pellets | 8.0 | 25 °C, 100 bar | [12] |

[a)] Calculated from density (0.21 g cm$^{-3}$) and pore volume (0.87 cm$^3$ g$^{-1}$).
[b)] Calculated from density (0.46 g cm$^{-3}$) and pore volume (0.65 cm$^3$ g$^{-1}$).
[c)] Room temperature

## Supplementary discussion for the anisotropic structures

As shown in Fig. 3a, the intensity of the sharp ZTC peak at $2\theta$ = 6.4° is diminished on the pressed surface after hot-pressing at 160 °C and 50 MPa in the presence of rGO, and disappears completely above 145 MPa. At the highest pressure explored (345 MPa), a broad peak appears at ca. 26° corresponding to the (002) reflection of graphitic carbon. Thus, the ordered structure of ZTC gradually collapses during the pelletization and a graphene-stacking structure is formed with increasing pressure. Interestingly, the XRD patterns of the cross-sections of the same pellets show very different effects, as shown in Fig. 3b. Even upon hot-pressing at the highest pressure (345 MPa), the ordered structure of ZTC remains, with a gradual decrease of d-spacing as witnessed by the shift of the (111) reflection to higher angle. The results of Fig. 3a and 3b are schematically summarized in Fig. 3c. Upon hot-pressing, the diffraction planes parallel to the pressing direction are retained, while the diffraction planes perpendicular to the pressing direction are destroyed. This anisotropy is evident not only in the ZTC ordered structure, but also in the GO stacking structure. Although GO can be reduced into rGO by the hot-pressing conditions as evidenced by Fig. S3, the cross-sectional XRD patterns of the resulting pellets still exhibit a broad reflection around 12° corresponding to GO stacking. Hence, some GO stacking which is parallel to the pressing direction is retained upon hot-pressing. These results indicate that both the ordered structure of ZTC and some of the GO stacking structure which are parallel to the pressing direction are retained during hot-pressing, forming a unique anisotropy in the resulting high-density graphene-like pellets.

## Supplementary discussion for the density of pellets

The $\rho_{max}$ of the pellets is apparently underestimated. There are two possible causes for this underestimation: the underestimation of $\rho_{skel}$ or overestimation of $V_{total}$ in Eqn. (1). Consider for example the case of ZTC_rGO_T300_P345 ($\rho_{bulk}$ = 0.98 g cm$^{-3}$, $\rho_{max}$ = 0.74 g cm$^{-3}$). The skeletal density, $\rho_{skel}$, of this pellet is 1.70 g cm$^{-3}$, which is lower than the density of graphite (2.26 g cm$^{-3}$) but consistent with numerous previous reports for pristine ZTC.[13,14] Nevertheless, it is possible that an underestimation of $\rho_{skel}$ could be a factor. If $\rho_{max}$ is calculated by using 2.26 g cm$^{-3}$ instead, the result becomes 0.83 g cm$^{-3}$. This value approaches the measured $\rho_{bulk}$ of 0. 98 g cm$^{-3}$, but is still smaller. Therefore, it is likely that $V_{total}$ is also overestimated. Under such an assumption, a minimum true value of the pore volume ($V_{total}$') would be calculated as 0.578 cm$^3$ g$^{-1}$ by Eqn. (1) using $\rho_{bulk}$ (0.98 g cm$^{-3}$) instead of $\rho_{max}$ and the skeletal density of graphite ($\rho_{skel}$ = 2.26 cm$^3$ g$^{-1}$). However, $V_{total}$' is still smaller than the measured value ($V_{total}$ = 0.76 cm$^3$ g$^{-1}$).

The above observations indicate that the ZTC/rGO pellets accommodate a much larger number of $N_2$ molecules than theoretically estimated. Such an enhancement in $N_2$ storage is expected to be highly advantageous for other gas storage applications (e.g., $H_2$ or $CH_4$ storage). One of the reasons for this enhancement effect may be the significant degree of adsorption-induced expansion observed in ZTC; this effect was recently described in detail elsewhere.[15] Briefly, when ZTC fully adsorbs water vapour, the framework expands to 108% of its original volume. If the same degree of expansion occurs upon $N_2$ adsorption, $V_{total}$' (0.578 cm$^3$ g$^{-1}$) is further increased to 0.62 cm$^3$ g$^{-1}$. This estimate is still smaller than the measured value (0.76 cm$^3$ g$^{-1}$).

## References

(1) Nishihara, H.; Yang, Q. H.; Hou, P. X.; Unno, M.; Yamauchi, S.; Saito, R.; Paredes, J. I.; Martínez-Alonso, A.; Tascón, J. M. D.; Sato, Y.; Terauchi, M.; Kyotani, T. A Possible Buckybowl-like Structure of Zeolite Templated Carbon. Carbon 2009, 47, 1220–1230.

(2) Marco-Lozar, J. P.; Kunowsky, M.; Suárez-García, F.; Carruthers, J. D.; Linares-Solano, A. Activated Carbon Monoliths for Gas Storage at Room Temperature. Energy Environ. Sci. 2012, 5, 9833–9842.

(3) Balathanigaimani, M. S.; Shim, W. G.; Kim, T. H.; Cho, S. J.; Lee, J. W.; Moon, H. Hydrogen Storage on Highly Porous Novel Corn Grain-Based Carbon Monoliths. Catal. Today 2009, 146, 234–240.

(4) Balahmar, N.; Lowbridge, A. M.; Mokaya, R. Templating of Carbon in Zeolites under Pressure: Synthesis of Pelletized Zeolite Templated Carbons with Improved Porosity and Packing Density for Superior Gas ($CO_2$ and $H_2$) Uptake Properties. J. Mater. Chem. A 2016, 4, 14254–14266.

(5) Kunowsky, M.; Marco-Lozar, J. P.; Oya, A.; Linares-Solano, A. Hydrogen Storage in $CO_2$-activated Amorphous Nanofibers and Their Monoliths. Carbon 2012, 50, 1407–1416.

(6) Jordá-Beneyto, M.; Lozano-Castelló, D.; Suárez-García, F.; Cazorla-Amorós, D.; Linares-Solano, Á. Advanced Activated Carbon Monoliths and Activated Carbons for Hydrogen Storage. Microporous Mesoporous Mater. 2008, 112, 235–242.

(7) Byamba-Ochir, N.; Shim, W. G.; Balathanigaimani, M. S.; Moon, H. High Density Mongolian Anthracite Based Porous Carbon Monoliths for Methane Storage by Adsorption. Appl. Energy 2017, 190, 257–265.

(8) Xu, B.; Wang, H.; Zhu, Q.; Sun, N.; Anasori, B.; Hu, L.; Wang, F.; Guan, Y.; Gogotsi, Y. Reduced Graphene Oxide as a Multi-Functional Conductive Binder for Supercapacitor Electrodes. Energy Storage Materials 2018, 12, 128–136.

(9) Kunowsky, M.; Suárez-García, F.; Linares-Solano, A. Adsorbent Density Impact on Gas Storage Capacities. Microporous Mesoporous Mater. 2013, 173, 47–52.

(10) Marco-Lozar, J. P.; Kunowsky, M.; Carruthers, J. D.; Linares-Solano, Á. Gas Storage Scale-up at Room Temperature on High Density Carbon Materials. Carbon 2014, 76, 123–132.

(11) Zacharia, R.; Cossement, D.; Lafi, L.; Chahine, R. Volumetric Hydrogen Sorption Capacity of Monoliths Prepared by Mechanical Densification of MOF-177. J. Mater. Chem. 2010, 20, 2145–2151.

(12) Purewal, J.; Liu, D.; Sudik, A.; Veenstra, M.; Yang, J.; Maurer, S.; Müller, U.; Siegel, D. J. Improved Hydrogen Storage and Thermal Conductivity in High-Density MOF-5 Composites. J. Phys. Chem. C 2012, 116, 20199–20212.

(13) Yang, Z.; Xia, Y.; Sun, X.; Mokaya, R. Preparation and Hydrogen Storage Properties of Zeolite-Templated Carbon Materials Nanocast via Chemical Vapor Deposition: Effect of the Zeolite Template and Nitrogen Doping. J. Phys. Chem. B 2006, 110, 18424–18431.

(14) Nishihara, H.; Hou, P.-X.; Li, L.-X.; Ito, M.; Uchiyama, M.; Kaburagi, T.; Ikura, A.; Katamura, J.; Kawarada, T.; Mizuuchi, K.; Kyotani, T. High-Pressure Hydrogen Storage in Zeolite-Templated Carbon. J. Phys. Chem. C 2009, 113, 3189–3196.

(15) Nomura, K.; Nishihara, H.; Yamamoto, M.; Gabe, A.; Ito, M.; Uchimura, M.; Nishina, Y.; Tanaka, H.; Miyahara, M. T.; Kyotani, T. Force-Driven Reversible Liquid–Gas Phase Transition Mediated by Elastic Nanosponges. Nat. Commun. 2019, 10, 1–10.